Scanning Electron Microscope Analysis of *Acanthocephalus dirus*

Physics 492R Capstone Project Report

Matheus Augusto Gabriel de Souza Menezes

A capstone project report submitted to the faculty of

Brigham Young University

In partial fulfillment of the requirements for the degree of

Bachelor of Science

Felipe Rivera, Advisor

Department of Physics and Astronomy

Brigham Young University

August 9, 2022

ABSTRACT

Scanning Electron Microscope Analysis of *Acanthocephalus dirus*

Matheus Augusto Gabriel de Souza Menezes

Department of Physics and Astronomy

Bachelor of Science

The purpose of this project is to produce publication quality microscopic images of spiny-headed worms, also known as thorny-headed worms, as well as to produce a reproducible and consistent method for obtaining consistent SEM imaging and EDX data regarding these specimens. The specimens studied are members of the species *Acanthocephalus dirus*, which was first described by Van Cleave in 1931 and revisited in the 1970s. This species belongs to the family Echinorhynchidae of the order Echinorhynchida. This order belongs to the class Palaeacanthocephala which is part of the phylum Acanthocephala of the kingdom Animalia. This species is a known parasite of various fish species, including but not limited to brown, brook, and lake trout (*Salmo trutta, Salvelinus fontinalis*, and *Salvelinus namaycush* respectively) as well as white bass and northern pike (*Morone chrysops* and *Esox lucius*, respectively). The images were obtained using the Helios Nanolab 600 Dual Beam scanning electron microscope which belongs to BYU's Electron Microscopy Facility. Scanning electron microscopy (SEM) and energy-dispersive X-ray analysis (EDX) were used to analyze surface structures and compositions. Hooks from the specimen were cross-sectioned using a Focused Ion Bean (FIB) to obtain the elemental chemical composition (via EDX) of their different layers. The images obtained convey the surface structure of various specimens of *A. dirus* with a particular focus on their respective proboscides. The images show that these specimens have 15 columns of thorns along their proboscides regardless of sex. EDX analysis identifies carbon, nitrogen, oxygen, sulfur, aluminum, phosphorus, magnesium, potassium, and calcium as the main components of the hook sheaths.

ACKNOWLEDGMENTS

Contents

List of Figures

List of Tables

1 Introduction

1.1 Motivation

The purpose of this research is to analyze and re-characterize the parasitic thorny-headed worms of the species *Acanthocephalus dirus*. They have been described previously, but without the aid of scanning electron microscopy (SEM), energy-dispersive X-ray analysis (EDX), and focused ion beam (FIB) sectioning. These technologies provide higher resolution and more detailed, more descriptive images than the ones obtained by light microscopes alone. In examining the surface structures and composition of the specimens of this species, we hope to provide more detail to its existing description and clearer images of the identifying features of *A. dirus*.

This is important because the taxonomic description of these parasites can be improved by the usage of electron microscopy, EDX, and FIB. *A. dirus* and other thorny-headed worm species have been identified, recombined, and redefined multiple times (see "Previous Research" below). Through this research, we can shed more light on the defining features of this species and identify its defining attributes so that taxonomic separation becomes clearer and more meaningful.

1.2 Background

Acanthocephalans are a group of species of parasitic worms, all of which have proboscides with hooks as a major defining characteristic of their anatomy. These hooks can be used to differentiate between species of thorny-headed worms. According to the Encyclopedia of

Life, there are more than 1300 known species of acanthocephalans, and most of them are parasitic to fish and birds, with a few being known to infect humans. The hooks characteristic of these species are the feature used to attach the parasites to the intestine of their hosts. These parasites lack a mouth or a digestive tract (Amin, 1975). Consequently, they are thought to be similar to cestodes which absorb nutrients through their tegument from the already digested food in their surroundings (Dalton, 2004).

The hooks, which define these parasites, may appear in differing numbers, shapes, sizes, and even chemical composition in different species of acanthocephalans. With little information available to describe these hooks to date, it can be difficult to characterize the similarities and differences between these parasites. Scanning electron microscopy can provide essential information about the physical structures of these parasites, necessary to clarify the similarities and differences, and help taxonomists classify these parasites properly (Amin, 2018). So far, studies have indicated that these hooks are similar to other mammalian hard tissues, such as teeth, and chemical analyses seem to confirm these findings, showing the presence of calcium, phosphorus, and sulfur (Amin, 2018). This paper aims to confirm these findings and provide additional information about these parasites, which would help complete the taxonomic picture of this branch of the animal kingdom.

1.3 Previous Research

Acanthocephalus dirus was first named and described through the efforts of Harley J. Van Cleave and Lee H. Townsend in 1931. At first, they decided to identify the species by the name *Echinorhynchus dirus* (Van Cleave, 1931). However, after 5 years, they wrote a paper explaining the need to change the genus assignment of this species from Echinorhynchus to

Acanthocephalus (Van Cleave, 1936). As such, they changed the name of this species to *Acanthocephalus dirus*. This name was unchanged until the 1960s and 70s when Dr. Omar Amin and Dr. Wilbur L. Bullock separately identified two new species which were then later combined into a more comprehensive definition of *A. dirus* (Amin, 1984).

Bullock et al. (1962) identified a new species of acanthocephalan under the name *Acanthocephalus jacksoni*. Amin et al. (1974) independently identified another species which was named *Acanthocephalus parksidei*. Amin et al. (1974) initially reported that *A. parksidei* looked like an intermediate between the specimens of *A. dirus* described by Cleave et al. (1931) and *A. jacksoni* described by Bullock et al. (1962). However, later research by Amin et al. (1984) redescribed *A. dirus* and combined these three species into one under the first name that was given to these parasites by Van Cleave et al. (1931).

Since the combination and description of these species, there has been little work done to recharacterize them. Although much has been studied concerning the life cycle and effects of these parasites on their hosts, the best images of any specimen available are either from light microscopes or line drawings. This paper aims to present SEM pictures and FIB/EDX analysis of several specimens of *A. dirus* and improve on previous descriptions of this species.

2 Methods

2.1 Equipment

The equipment used for this research consists of the Helios Nanolab 600 Dual Beam scanning electron microscope with EDX and FIB capabilities.

Figure 2.1 Helios Nanolab 600 Dual Beam scanning electron microscope

2.2 Sample Preparation

The objective of sample preparation is twofold. The first is to preserve the natural structure of the sample as much as possible. The second is to create a sample that can be studied under the conditions of the electron microscope. Chemical preparation, fixation, and critical-point drying, address the first of these objectives through the procedure outlined in sections 2.2.1. and 2.2.2 and in section 2.2.2.

2.2.1 Chemical Preparation

2.2.1.1 Sample acquisition

a. The sample to be studied should be as fresh as possible. In the ideal scenario, it is still alive when placed in the primary fixative chemical, which will kill the sample.

b. The sample should be small. If necessary, dissection of the sample to fit the size requirements should be performed. For this project, anything that fits well within the boundaries of the SEM mount is considered small enough (~1cm). All the *A. dirus* specimens received fit into the mounts well, so no dissection was needed.

2.2.1.2 Primary fixation

a. The standard is to use 2% glutaraldehyde in 0.06M sodium cacodylate buffer as the primary fixative. The buffer is used to protect the sample from the full effect of the primary fixative, which can be quite harsh and compromise the structure of the sample. It also controls pH and osmolarity of the environment the sample will be in order to mitigate structural damage.

b. The sample should be in the primary fixative for at least 2 hours. The sample can be stored in the primary fixative for weeks if necessary. However, the best results come from completing the sample preparation procedure as soon as possible.

c. The sample should be centrifuged, and any particulates left in the supernatant washed off since they can interfere with the following steps of the procedure.

d. After fixation, the sample should be put on filter paper, and waste chemicals disposed of as appropriate.

2.2.1.3 Wash samples

a. Wash samples with buffer to remove any unreacted fixative that might be left over. To do this, remove the primary fixative and add the buffer, letting it sit for

5-10 minutes. Then, repeat this process 5-6 times. Then get rid of waste chemicals appropriately.

2.2.1.4 Secondary fixation (Optional)

a. For the secondary fixation, 1% osmium tetroxide with buffer should be used. Ideally, the sample is placed in this fixative for at least 1.5 hours but no more than 2 hours unless otherwise indicated.

    i. Osmium tetroxide is highly toxic. use only under a functional fume hood and dispose of it appropriately. Refer to its safety material data sheet for more information.

2.2.1.5 Secondary wash

a. Wash the sample following the previous procedure using distilled water instead of buffer.

2.2.1.6 Dehydration in ethanol or acetone

a. We use a series of washes of different dehydrator concentrations to remove any water left over on the sample. The leftover water can cause holes and affect imaging when the sample is placed under a vacuum, so it is paramount to remove it completely.

b. Dehydration is done by following the wash procedure outlined above with increasing concentrations of ethanol. For Acanthocephala, we use 10%, 30%, 50%, 70%, and 95% once for 5-10 minutes each and 100% for 5-10 minutes three times.

After the third wash in 100% ethanol, all the water in the sample should have been replaced by ethanol. This ethanol should be removed using the next step in the sample preparation procedure, which is critical point drying.

2.2.2 Critical Point Drying

To preserve sample morphology, critical point drying is the state-of-the-art method found for these types of specimens. At the critical point, the physical characteristics of liquid and gas states are indistinguishable. Compounds that are at the critical point can be converted between the liquid and gaseous phases without passing through the interfaces between liquid and gas states, thereby avoiding the damaging effects of this transition. The dehydration of the samples using the critical point of water is not feasible since it lies at 374 °C and 229 bar where any biological sample would be destroyed. To overcome this problem, water can be replaced with liquid carbon dioxide (CO_2), whose critical point lies at 31 °C and 74 bar. This is more appropriate for all biological applications and relatively easy to maintain.

However, CO2 has one serious disadvantage as a transitional fluid: it is not miscible with water. Therefore, water has to be replaced by exchange fluids like ethanol or acetone which are miscible in both water and liquid CO_2, which was accomplished through the sample preparation procedure outlined above. Still, CO2 needs to be used for critical-point drying the triple points for both ethanol and acetone are found at undesired temperatures/pressures (Ethanol: Pc 60 bar/Tc 241 °C; Acetone: Pc 46 bar/Tc 235 °C). After replacing water with an exchange fluid in a pre-critical point drying step and in turn replacing this exchange fluid with liquid carbon dioxide, the liquid CO_2 is brought to its critical point and converted to the gaseous phase by decreasing the pressure at the constant critical point temperature.

To do so, open the critical point dryer and place the sample inside along with the spacer to limit CO_2 waste. Then, close the dryer and tighten the bolts around the lid one at a time following a star pattern, making sure they are all tightened a little before tightening them completely. Make sure that the bolts are tight because there could be CO_2 leaks if the lid is not closed properly.

Then turn on the critical point dryer for 4 cycles (which will last 8 hours) and come back the next day. After the cycles on the critical point dryer, all the ethanol and CO_2 should be removed from the sample. The ethanol should have been replaced by the CO_2 and the CO_2 should have transitioned to the gaseous phase beyond the critical point, preserving sample structure and preventing damage. However, though this prepares the sample to preserve its structure while in a vacuum environment, it does not prepare it to be imaged under the electron beam as biological samples tend to be non-conductive. To address this issue, the sample needs to be coated in a layer of conductive material that provides a path to electrical ground for the electron beam and facilitates image production. To do that, the sputter coater should be used.

2.2.3 Sputter Coating

Biological samples are non-conductive, and non-conductive samples often have a charging effect caused by electrons collecting on the sample surface, which produces various issues and artifacts while imaging in the SEM. Some SEM systems have "low vacuum" or "charge reduction" modes that can mitigate these issues, but those modes have magnification and image quality limitations that depend on the sample under scrutiny. In addition, images produced using these modes usually have a flat contrast and become unappealing.

To better image the surface features of non-conductive samples at the spatial resolution SEMs can provide, non-conductive samples are commonly coated by using a sputter coater that creates a nano-thin layer of conductive metal around the sample. Even conductive samples benefit from a sputter-coated layer of materials with abundant potential for electron emission. In our case, the chosen material for sputtering is a mixture of gold and palladium (80-20). This coating allows imaging at the higher beam energies necessary to reach the highest resolution and magnification without concern of electron charge effects or beam damage to sensitive samples.
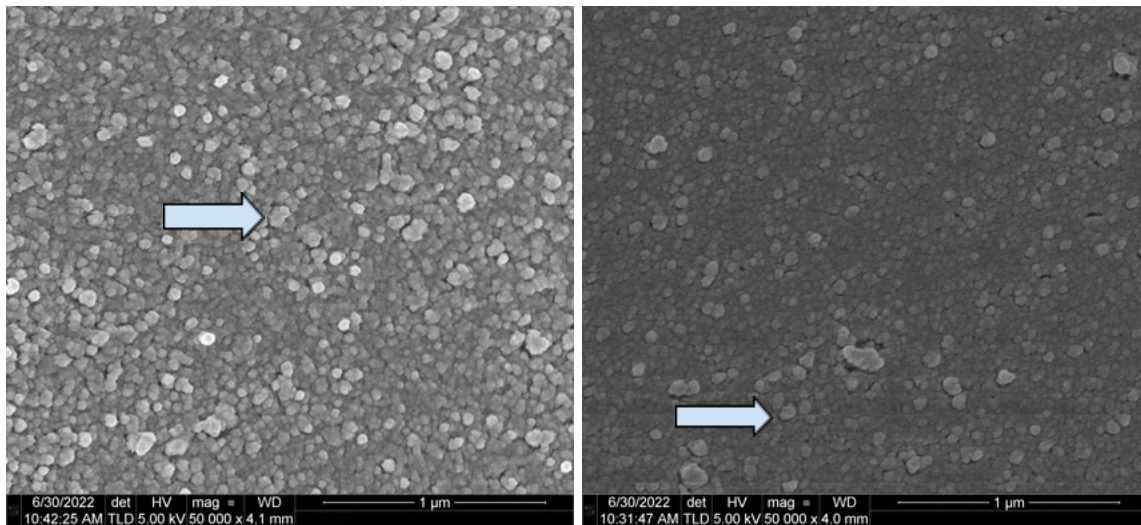
Fig 2.2 Electron charge effects cause the lines visible in the above images. They are horizontal and cross the images at various spots. Posterior integument (left) and anterior integument (right) with charging lines

EDX analysis can still be done on coated samples as most EDX software allows for the definition of the coating metal so that it is ignored during analysis. If that is not possible, the analyst can define the coating material and ignore it after analysis. With some knowledge of the sample under preparation, a metal coating type that is not present in the sample may be selected.

9

This is the reason why a mixture of gold and palladium was selected to coat our *A. dirus* specimens.

Since the level of vacuum plays a role in the resulting grain size, it was necessary to use a High Vacuum coater for the production of clear images at 50,000X magnification with the aid of Field Emission or FE-SEM where the potential exists to observe the artifact of coating grains.

The sputter coating chamber we used is a self-contained computer-controlled unit (Quorum Q150TES). To successfully operate the sputter coater, we used the procedure outlined below from 2.2.3.1 to 2.2.3.10.

2.2.3.1 Open the black nitrogen tank valve

2.2.3.2 Run the vent process (QT vent chamber) present in the sputter-coater display screen.

2.2.3.3 Check recipe for coating procedure

    a. If necessary, edit the profile. Certify that the 90-second timed deposition is selected and choose stage rotation for acanthocephalan specimens.

    b. With stage rotation, make sure that the stage is balanced with a counterweight, similar to the procedure necessary to preserve the integrity and functionality of a centrifuge.

2.2.3.4 Choose stage

    c. The options are "flat" or "tilt"

        i. For our purposes, a tilted stage was used, and the proper counterbalance weight was placed on the opposite side of the stage.

2.2.3.5 Add sample(s) to stubs/mounts using double-sided conductive tape

2.2.3.6 Mount the stubs onto the stage for the coating process.

2.2.3.7 Run vacuum process until completed (takes a couple of minutes)

2.2.3.8 Run recipe (e.g. AuPd Timed Process) until completed

2.2.3.9 Run vacuum shutdown process

2.2.3.10 Turn off the black nitrogen tank valve

2.3 Image Collection (SEM)

The signals used by an SEM to produce an image result from interactions of the electron beam with atoms at various depths within the sample. For basic image production – the main focus of this research – the most important signal is the one resulting from secondary electrons (SE).

Secondary electrons (SEs) have low energies on the order of 50 eV. This limits their mean free path when traveling through solid matter. Consequently, SEs can only escape from the surface with a volume of just a few nanometers below the surface of a sample. The SE signal has a tendency to be highly localized at the point of impact of the primary electron beam, making it possible to collect images of the surface of the sample with a resolution better than 1 nanometer.

To successfully operate the microscope, it is necessary to follow the procedure described in 2.3.1 and 2.3.2.

2.3.1 Startup procedure

2.3.1.1. Check color indicators

a. Verify that the vacuum and electron beam source color indicators are green. They are located at the top and bottom right of the main screen of the monitor controlling the microscope.

2.3.1.2 Vent system

    a. Press the "Vent" button on the top right and confirm. Wait for the vacuum color indicator to turn gray. It takes 5-8 minutes to vent.

    b. While venting, make sure that the stage is set to the programmed Sample Exchange Position by navigating to the stage menu, selecting "Sample Exchange Position" from the menu, and pressing "Go To."

2.3.1.3 Open microscope door

    a. The "negative pressure" of the vacuum keeps the door closed when the microscope is in use, so there are no locks or bolts that keep the door closed.

2.3.1.4 Load the sample onto the stage

    a. Wearing the clean gloves provided, use the screwdriver to secure the mount onto the stage by tightening the holding screw and making sure that the mount does not rotate. (Do not excessively tighten the screw. It is made of steel and the mount is aluminum. Excessive tightening will cause damage to the sample mount).

2.3.1.5 Check sample height using the available gauge

    a. The gauge is a rectangular piece of solid metal with an overhang that permits height measurements. Make sure that the height of the tallest spot on the sample falls between 4 and MAX on the indicator. If necessary, adjust sample height by loosening the cone at the base of the stage and by rotating the stage clockwise or counterclockwise.

2.3.1.6 Take note of the position (hole) in which the sample was loaded.

a. The holes are numbered from 1 to 14. There is no indicator afterward on the monitor or the camera to verify the chosen holes. Taking note will save the time necessary to vent and pump the system once more for verification.

2.3.1.7 Gently close the microscope door and pump down the system

a. Hold the microscope door closed and press the "Pump" button on the top right. Hold until the roughing pump noise is heard from the adjacent room.

2.3.1.8 Move the stage

a. While the system pumps down, move the stage to the desired position by selecting the stage menu and selecting the hole your sample is in, unchecking the z-distance box, and clicking "Go To".

b. During this time, also check the beam settings to make sure they are set to the desired values. For acanthocephala analysis, we use the ETD (SE) Detector. If this is not the selected setting, click the button that contains the picture of an eye on the top right and change it to the correct setting.

2.3.1.9 Check vacuum indicator

a. Wait until the vacuum indicator on the bottom right turns from yellow to green. This should take between 5 and 8 minutes.

b. DO NOT press the "Wake Up" button unless using the ion beam.

2.3.1.10 Turn on the electron beam

a. Press the "Beam On" button. There will be a popping noise from the microscope that indicates the beam is turning on. Standard Imaging parameters for these samples include a beam potential and current are 5kV and 86 pA, respectively. We

also use the 100 ns dwell time to look for the desired image locations. These

settings are what we used for the general images of the acanthocephalans.

2.3.1.11 Navigate to the point of interest in the sample

a. Using the available controls (central button click and drag, double click, or by

drawing a rectangular box), find the desired image location. Remember that the

view on-screen is from the point of view of the right side of the microscope and

navigate accordingly.

2.3.1.12 Rough focusing

a. Once at a point of interest, go to 1,000X+ to focus the microscope on your

sample reasonably well.

b. To focus the microscope this first time, use the coarse and fine focus

knobs on the right of the dial board above the keyboard.

2.3.1.13 Link the distance between the sample and the emitter

a. Once in focus, link the distance from the stage to the emission tip by clicking the

link distance button. It has a blue microscope icon with a red question mark. It

says "link distance" when you hover over it.

2.3.1.14 Set the sample at eucentric height

a. With the distance linked, go to the stage manipulation menu and move the z

distance to 4 mm, which is the eucentric distance of this microscope. Do this by

checking ONLY the z-distance box, inputting the value 4 in the box, and clicking

"Go To". Watch the stage move using the CCD on the bottom right display panel.

If it gets too close to the tip or if it seems worrisome, you can stop stage

movement by clicking the "Stop" button at the top while the stage moves. (The "Go to" button turns into the "Stop" button during stage movement).

b. When the specimen is placed correctly at the eucentric height and the stage is tilted, the point you are observing remains stationary. It also allows for better image resolution and focus.

2.3.1.15 Refocus

a. Once at 4 mm, refocus the beam (again above 1,000x), relink the distance, and move the z-distance back to 4 mm.

After the startup procedure is completed, the sample is at the correct place to produce the sharpest images possible when imaged.

2.3.2 Basic SEM imaging

2.3.2.1 Improve focus and correct for astigmatism

a. To take a crisp, clear picture, the focus obtained with the startup procedure is not accurate enough. To improve focus, magnify to approximately 4 times the magnification of the desired picture (For example, if the desired picture magnification is 10,000x, then find focus at 40,000x+).

b. Once magnified, use coarse and fine focus knobs to improve the image as much as possible. This might be difficult because the stigmators will probably be in the incorrect setting.

c. When the focus cannot be improved, then use the stigmators to clarify your image.

i. To do this, choose one stigmator knob (either x or y) and spin it in both directions until you find the clearest image in between the blurry ones. To find astigmatism, look for blurriness that follows along any axis, not necessarily a horizontal or vertical one. Once you find this in both directions of knob spinning, find the best image in the middle (the one that has the least blurriness along either axis).

ii. One tool that can be helpful here is the reduced area button. With the same time settings, the reduced area will produce an image with less noise, making it easier and faster to identify astigmatism and correct it.

Reiterate the focusing process until the background of your image at 4 times the desired magnification is the clearest. Then, zoom back out to the desired magnification and take the picture. Be careful not to move the sample, especially if it has considerable topographical features. Focusing depends on the distance of the sample to the tip, and if the sample is moved, refocusing will be necessary.

2.4 Sectioning (FIB)

A focussed ion beam (FIB) will damage the sample while imaging or milling, thus, only use the Focused Ion Beam sectioning feature after all the desired SEM micrographs of the intact specimen have been taken. The ion beam damages the sample and images of the sample, after milling or imaging with the FIB, will be compromised.

A focused ion beam (FIB) instrument is similar to a SEM, but uses a beam of ions rather than electrons. The focused ion beam can directly modify or "mill" the sample surface via a sputtering process. This milling can be controlled precisely down to the nanometer scale. With

careful control of the intensity and energy of the ion beam, it is possible to conduct precise

nano-machining to produce minute components or to remove unwanted material from a surface.

To operate the FIB properly, it is necessary to follow the procedure outlined below.

2.4.1 Focused Ion Beam Manipulation

2.4.1.1 Remember that the ion beam is always milling.

2.4.1.2 Ensure that the sample is at the microscope's eucentric height

a. Before turning on the ion beam, make sure that your sample is at the eucentric

height and at the correct position to be milled. For the Helios Nanolab 600 Dual

Beam, the sample should be approximately 4 mm from the emission tip and tilted

at a 52 degree angle so that the ion beam hits it straight on at an angle of 90

degrees.

i. To place the sample at the correct position, first find eucentric with the

startup procedure. Then, find a recognizable, distinguishing feature and

place it in the center of your electron beam display on the top left.

Afterward, go to the stage manipulation menu and perform a 5-degree

rotation while following that distinguishing feature with your eyes.

ii. You should notice that the distinguishing feature moved somewhere either

above or below the center of the top left panel (i.e. the panel selected to

show the ion beam image) where it was located before the tilt. To find it

again, select the CCD display on the bottom right and use the center

button press and drag technique to move the stage either up or down the

necessary amount to center the same distinguishing feature again.

2.4.1.3 Rotate Sample

    a. Once the same distinguishing feature has been centered again, rotate the sample to 52 degrees and repeat the above procedure to center it. Rotation can be performed repeatedly from 0 degrees to 5 degrees and to 52 degrees to make sure the sample stays centered after rotation, but the microscope is not perfect. Due to mechanical adjustment limitations, true eucentric will always be a little elusive, so if the distinguishing feature stays pretty close to the center during and after rotation, that was considered enough for our purposes.

2.4.1.4 Adjust contrast

    a. Once the sample is at eucentric and rotated to 52 degrees, increase the contrast of the electron beam to be able to see the image more clearly. The rotation causes more electrons to be emitted away from the detector, so the total signal will decrease, and the image will become darker. Increasing the contrast solves this issue.

2.4.1.5 Turn on the FIB source

    a. Turn on the ion beam by clicking the "Wake up" button and waiting for the source color indicator to turn green

    b. This step can take a while. When we became comfortable and efficient at finding eucentric for the ion beam, we started this step before the iteration of steps 2, 3, and 4 so that the source is ready when you finish centering the sample.

2.4.1.6 Turn on the FIB

    a. Once the source goes green, turn on the ion beam to be able to see and mill with it.

i. DO NOT leave the ion beam on over your sample. If you need to see the sample using the ion beam, use the "Snapshot" feature of the ion beam instrument to adjust imaging position underneath it, and monitor by using electron beam snapshots. Shift+right click shift the ion beam.

  1. The ion beam interferes with electron beam imaging by producing more secondary electrons, so using snapshots of both the electron beam and the ion beam will give you clearer images to see what's happening while preserving your sample from unnecessary milling.

2.4.1.7 Create a protective layer (optional)

Ion beam-assisted chemical vapor deposition can be used to deposit metals with precision similar to FIB milling. In our case, a small quantity of a platinum metal-organic gas can be injected into the vicinity of the beam, where exposure to the beam will decompose it. Deposition of the nonvolatile decomposition products on the specimen surface would then happen while the volatile products would be extracted by the vacuum system.

It should be noted that for our current acanthocephalan analysis, depositing a protective layer does not provide enough benefit to be worth the cost. However, future analysis of surface features may require it. The procedure below is presented for that use case.

a. Draw the desired pattern of deposition using the ion beam deposition and milling menu on the top right. Different milling and deposition patterns can be selected, but we will only use a rectangle and the two cross-section settings

b. To deposit, select the Pt deposit setting on the material, then warm up the source by double-clicking the "Cold" indicator. After the bar charges up to full and the

indicator says "Warm," leave it on warm for a couple of minutes to ensure that the source doesn't cool down drastically during deposition.

c. Then, insert the Pt depositing needle by checking the box all the way to the left (on the same line whose indicator should now say "Warm"). Then confirm deposition on the pop-up box.

d. Before depositing/milling, verify the settings of the beam (i.e. current and voltage) and change them to ensure a depositing time between 3 and 10 minutes. Doing it any faster creates the risk of incorrect milling and material re-deposit, while any slower compromises efficiency.

e. Always use the top selection of the duplicate values for ion beam current for anything. In addition, double-check the actual beam current on the bottom right, which shows up close to the vacuum pressure.

f. When the needle is inserted, don't move the stage.

g. Ion beam current strength depends on the area of deposition. We aimed to have 6-10 pA per square micron and tried to stay toward the lower end of that range.

2.4.1.8 Select material to be milled

a. For Acanthocephala and other biological applications, we used the PMMA cutting setting to make it work. This is the most similar material to the biological consistency of the parasites under scrutiny.

i. Note that, although PMMA is the most similar material to our biological samples, it is not identical. With the PMMA setting selected, the ion beam will mill further than the setting chosen. For example, if the beam is

programmed to mill PMMA down 1 micron, it will mill our biological

sample further than that, closer to 1.5-2 microns.

After milling, verify that only the desired portion of the sample was milled away.

Depending on the structure, composition, and beam settings, the damage to the sample might be

greater than expected, and new patterns will have to be made. However, if done correctly, the

cross-sections produced by the FIB can now be analyzed by EDX. We used a regular

cross-section with the PMMA setting and milled a 45-micron by 25-micron box down to a depth

of 3 microns using a current of 2.7 nA, which resulted in a milling time of approximately 11

minutes. This was then followed by a cleaning cross-section pattern at 90 pA that took another 8

minutes and produced the following image.

Figure 2.3 Longitudinal cross-section of a middle hook of a female specimen of *A. dirus*.

2.5 Analysis of Hook Composition (BSE and EDX)

Another signal that can be detected when scanning the surface of a prepared sample with

an electron beam is that of back-scattered electrons. Back-scattered electrons (BSE) are beam

electrons that reflect back from the sample by elastic scattering. They have significantly higher energy than secondary electrons, so they emerge from deeper locations within the specimen. Therefore, the resolution of BSE images is lower than that of secondary electron (SE) images. However, BSEs provide another use in SEM. Along with the spectra made from the characteristic X-rays, the BSE signal intensity can be used to identify the chemical composition of a sample because that intensity is strongly related to the atomic number of the specimen. BSE images provide information about the distribution of different elements in the sample. In our research, the samples are predominantly composed of light elements because they are biological specimens, and BSE imaging can identify these elements which would otherwise be difficult or impossible to detect in secondary electron images.

Further, X-rays are produced when the electron beam interacts with the sample, thus, they generate yet one more additional signal that can be detected in the SEM. Characteristic X-rays are emitted when the electron beam dislodges an inner shell electron from the atoms in the sample, causing a higher-energy electron from a higher shell to fall into the lower shell and release energy. The energy and frequency of these characteristic X-rays can be measured by energy-dispersive X-ray spectroscopy (EDX) and used to identify and measure the abundance of elements in the sample and map their distribution.

To use the Helios EDX function, we followed the procedure outlined below.

2.5.1 Energy-Dispersive X-ray Analysis (EDX)

2.5.1.1 Turn on TEAM software

a. TEAM is the software used for EDX analysis on the Helios. Log in with the credentials provided and select the correct project. In our case, that project was the Heckman project for acanthocephala.

2.5.1.2 Verify apparatus status

a. Look at the icon on the bottom right of the monitor that controls the EDX machinery. If it is green, then continue onto the next step. If it is red, select it and turn on the cooling. This is necessary to prevent any damage that might happen from overheating.

2.5.1.3 Adjust photon count

a. Verify the photon count on the bottom left of the monitor. If the CCD that is used to monitor the stage and the inside of the microscope is on, the photon count will be too high for effective analysis , more than 100,000 counts per second. Therefore, pause the CCD to lower the infrared photon count to around 10,000 counts per second, increase dead time and reduce X-ray noise to facilitate analysis.

2.5.1.4 Adjust electron beam settings

a. The typical values for EDX signal analysis are very different from the settings used for SEM basic image acquisition described in section 2.3. In general, voltage values for EDX should be two to three times above the necessary voltage to excite the highest expected characteristic X-rays. For acanthocephalans, the voltage we used was 15 kV.

2.5.1.5 Move sample to the correct height

a. The specimen needs to be at eucentric height to optimize detectable X-rays from the electron beam interactions. These emitted rays travel in straight lines and the detector is in a fixed location. Follow the procedure outlined in 2.4.1 to position the sample correctly.

2.5.1.6 Change the mode of the microscope and the detector in use

a. Change the mode of the microscope by clicking on the mode menu and selecting "SEM mode 3 - EDX." This envelops the sample in a magnetic field and improves the signal at the detector, resulting in a more accurate analysis.

b. Change detector to "TLD" instead of "SE." This activates the fixed EDX detector and allows for analysis.

2.5.1.7 Adjust "dead time"

a. We wanted the "dead time" to be around 30% to allow time for the analysis and characterization of each acquired X-ray emitted by the sample as a result of the electron beam interaction. The values chosen for our EDX analysis varied between 60 picoamps and 2.7 nanoamps.

2.5.1.8 Focus

a. Unlike basic imaging, EDX analysis does not require exact focus. We simply made sure that the sample was visible enough to clearly indicate where the X-rays originated.

2.5.1.9 Set collection bin size

a. The resolution of the energy characterization of the detected X-rays has a limit of 5eV, so set the bin size to that. This will cause the system to record the detected X-rays as if in a histogram, with energies that increase discreetly by 5eV per bin

and reporting a count of how many X-rays of those energies were received by the detector.

2.5.1.9 Set collection time

a. For our purposes, we used 30 seconds of collection time per run. This was sufficient for our purposes, but if more accurate data is needed, the collection time should be increased by raising the order of magnitude to the power of two. For example, if we were unsatisfied with the data using 10 seconds of collection time, we should increase the time to 100 seconds to improve the data

    i. Collection time does not include dead time. If the collection time is set to 100 seconds and the dead time is 30%, expect the collection to take closer to 143 seconds.

2.5.1.10 Identify possible elements present

a. Using the special periodic table provided by the program, we chose the most likely elements to be present in the sample. Those include C, N, O, P, S, Fe, Na, Au, Pd, Ga, Mg, K, Ca, and Al. We had special interest on the presence of sulfur, calcium, and phosphorus because those seemed to be the most prevalent elements in different species of acanthocephalans.

    i. We selected gold, palladium, and gallium because those are the materials needed for the sputter coater and by the ion beam. If those were suspected to be in the sample, we would have used a different metal coating with a different source for the ion beam.

2.5.1.11 Collect data

a. Using the reduced area button, we selected various spots along the cross-sections of the hooks to determine their composition and possible variations that would depend on location along the hook. Chemical compositions were determined for 3 spots along 2 different hooks: the tip, the middle, and the base, with the base being the spot where the hook goes into the proboscis of the parasite.

Collected data is reported in the next section.

3 Results, Discussion, and Conclusion

3.1 Results

Learning and following the procedures outlined in the methods section allowed us to take the following pictures. They will be split into sections by the determined sex of the specimen and further by sections of the specimen.

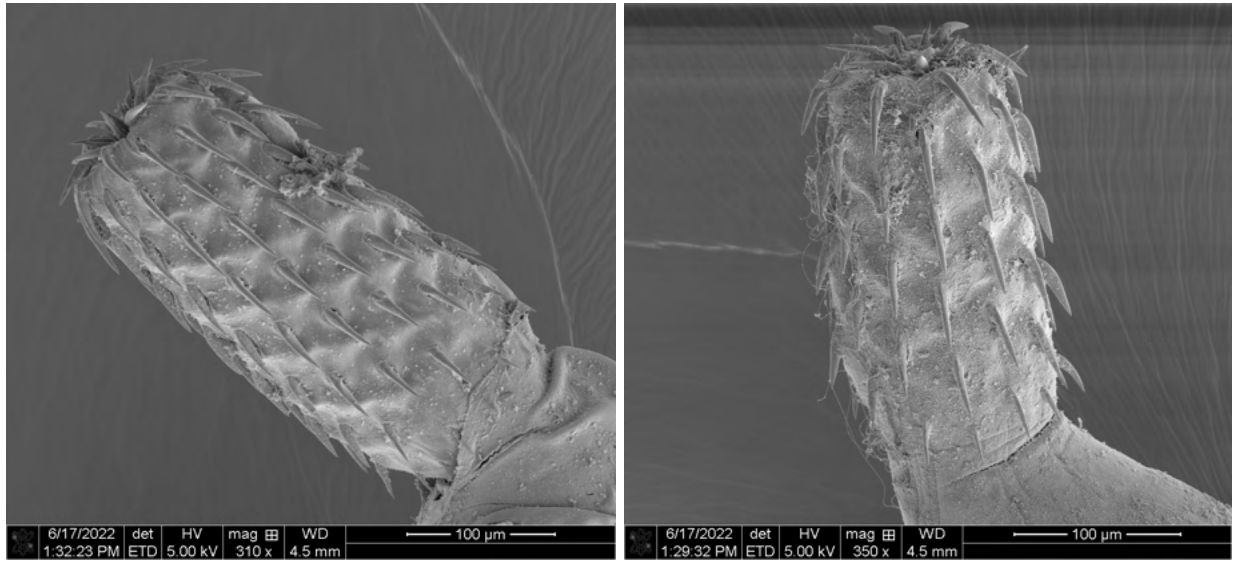### 3.1.1 Scanning Electron Micrographs of the Acanthocephala Males
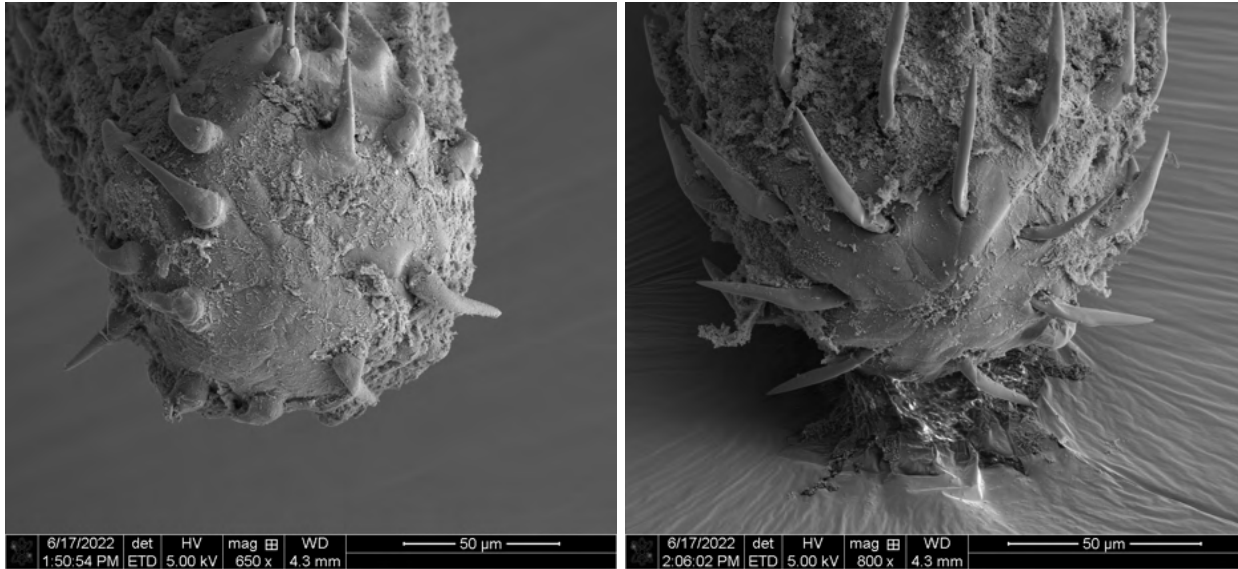
3.1.1.1 Proboscides
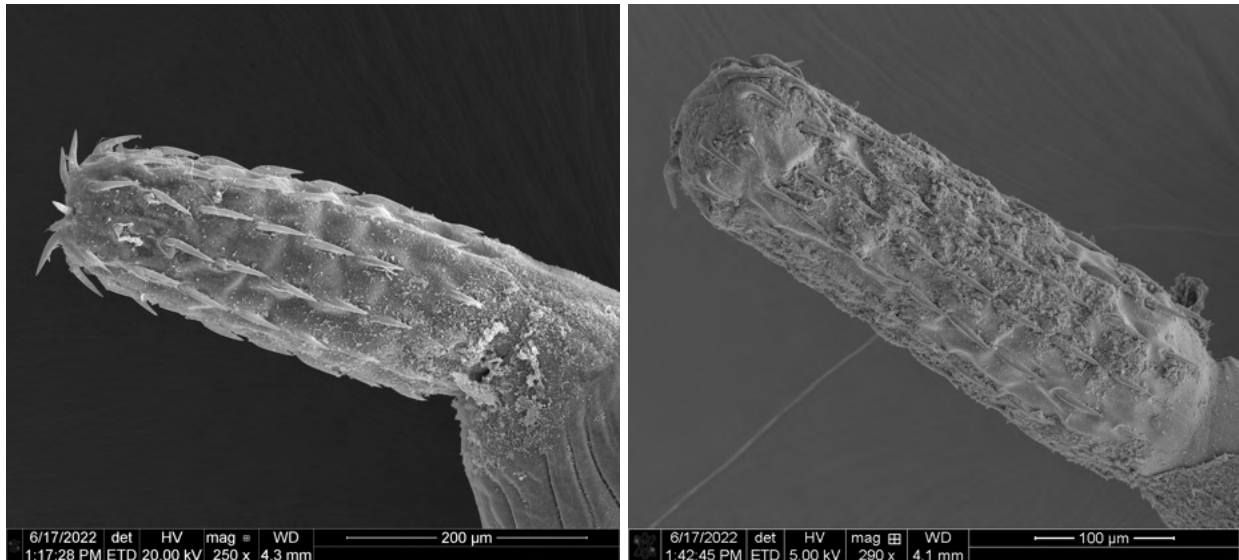
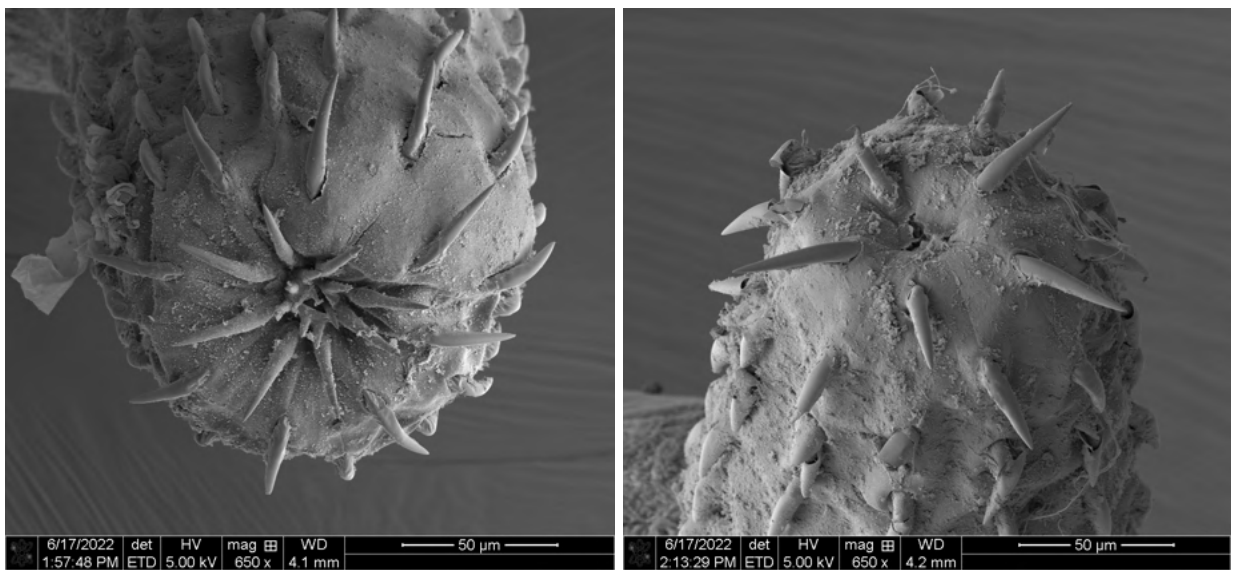**Figure 3.1** Lateral view of fully everted proboscides from male specimens of *A. dirus*.
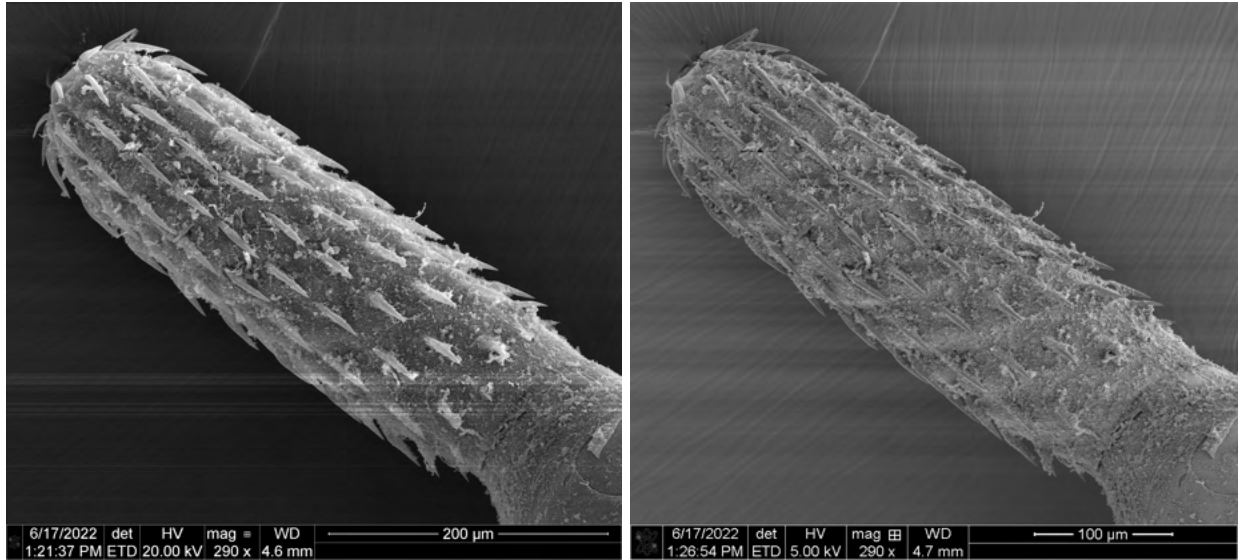
Figure 3.2 Additional lateral view images of fully everted proboscides from male specimens of *A. dirus*. Note the charging lines on both pictures.

Figure 3.3 Lateral view of partially everted proboscides from male specimens of *A. dirus*.
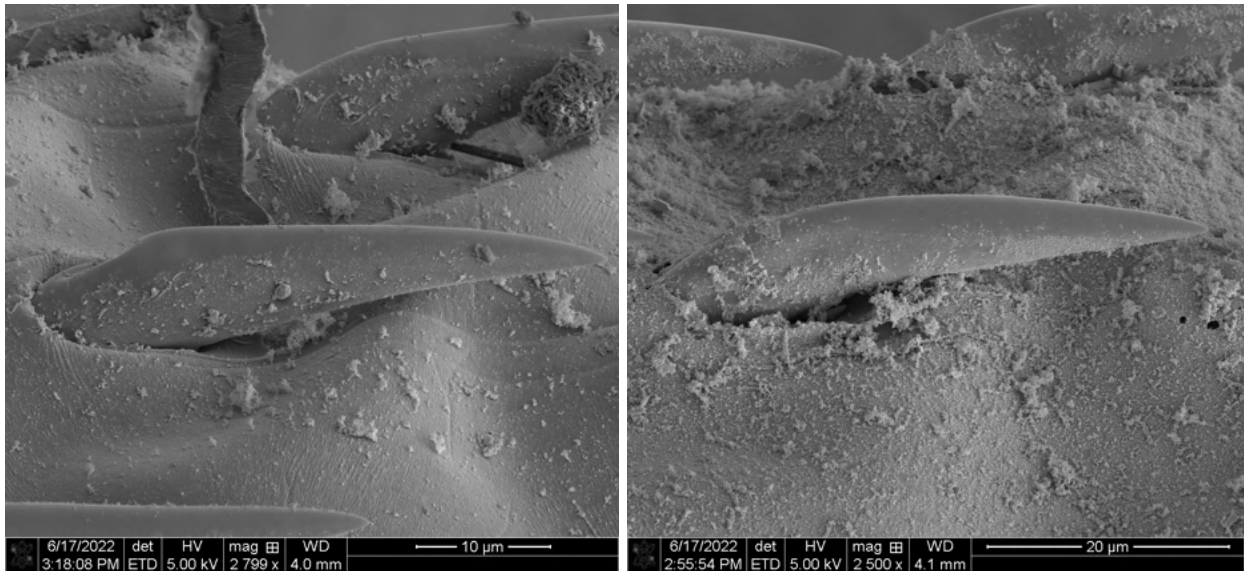
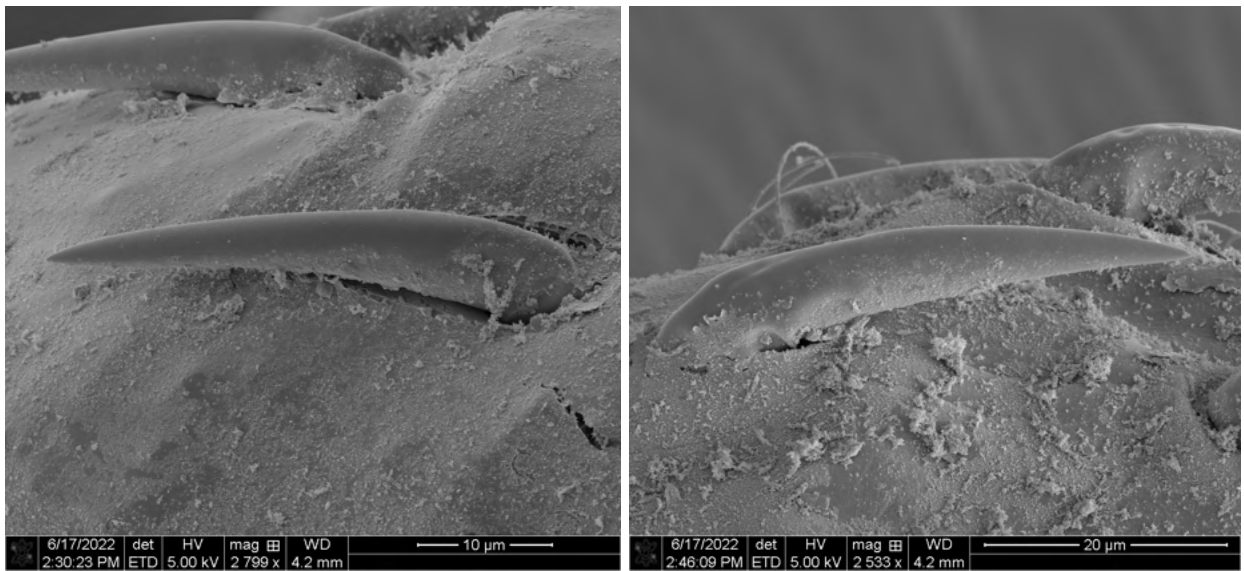**Figure 3.4** Anterior view of fully everted proboscides from male specimens of *A. dirus*.

Figure 3.5 Anterior view of partially everted proboscides from male specimens of *A. dirus*.
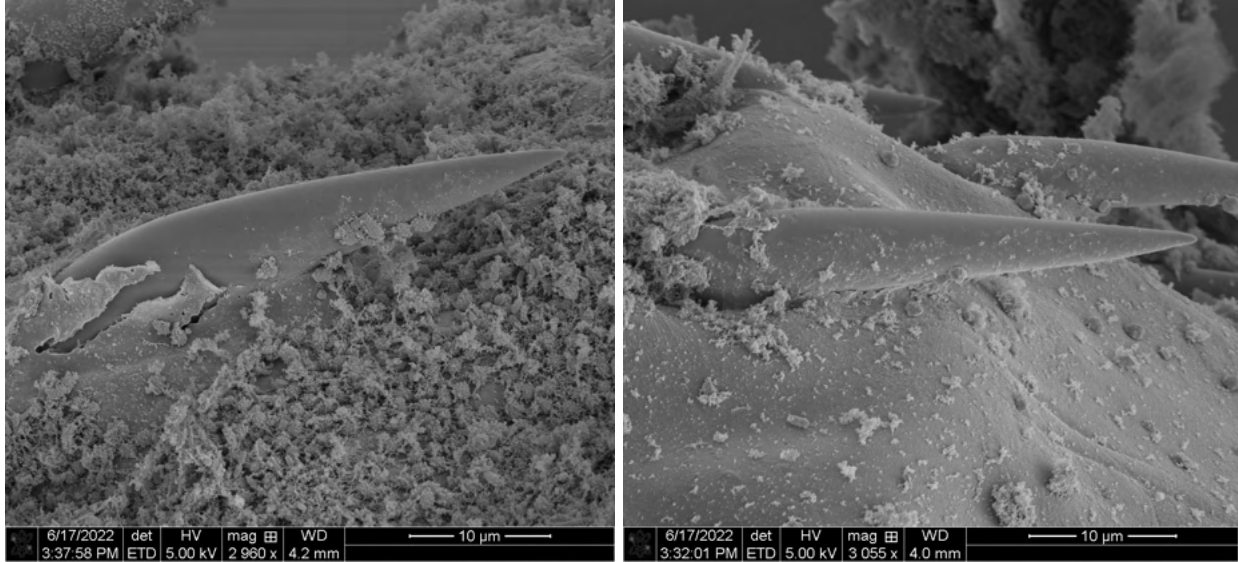
3.1.1.2 Hooks

Figure 3.6 Lateral view of anterior hooks from male specimens of *A.dirus*.

Figure 3.7 Lateral view of middle hooks from male specimens of *A.dirus*.

Figure 3.8 Lateral view of posterior hooks from male specimens of *A.dirus*. Note the size difference between anterior, middle and posterior hooks

3.1.1.3 Pores

Charging effects prevented the production of clear images of the pores along the proboscis and integument of the males. The best images collected are presented below.
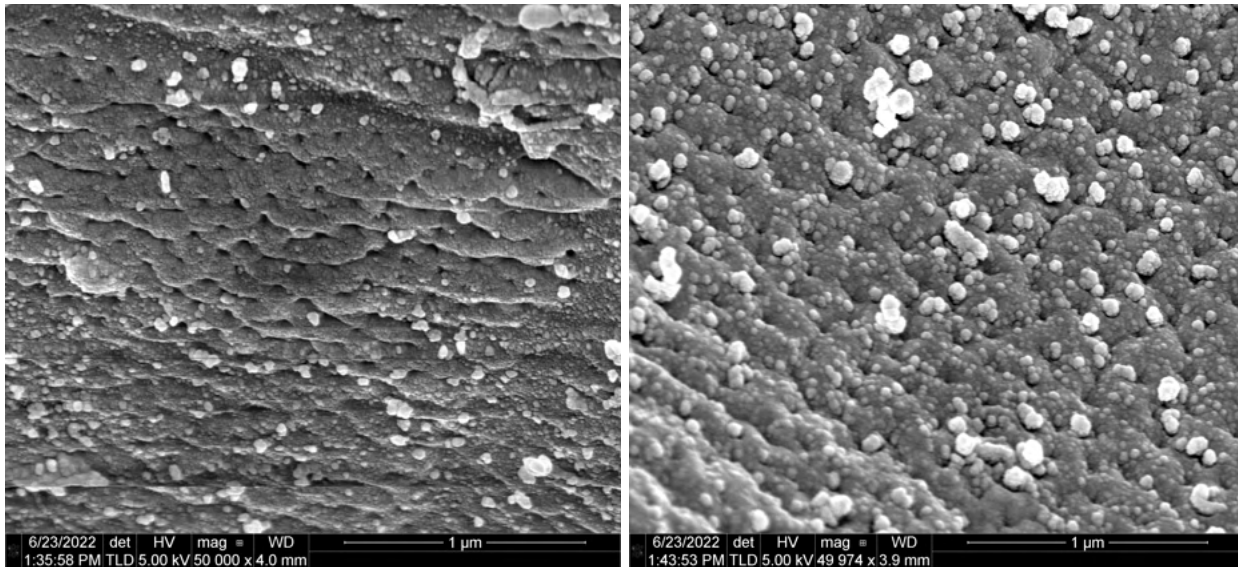
Figure 3.9 Pores on the proboscides of male specimens of *A. dirus*. Note charging lines and depth of focus issues on both pictures.

3.1.1.4 bursae

Figure 3.10 Lateral view of bursae from *A. dirus*.

Figure 3.11 Anterior view of bursae from *A. dirus*.

a. Bursa suckers. Examples of these structures can be seen as the two disks visible toward the bottom left corner of the left image of Figure 3.10. The following images zoom in to characterize them better.
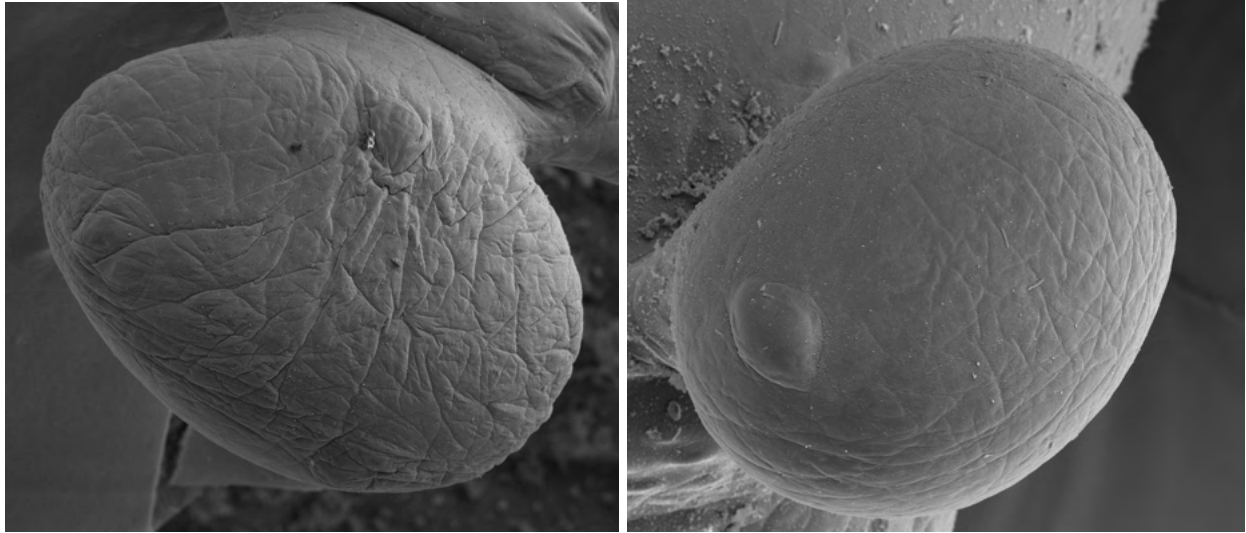
Figure 3.12 Bursa suckers from specimens of *A. dirus*.

3.1.2 Scanning Electron Micrographs of the Acanthocephala Females

3.1.2.1 Proboscides
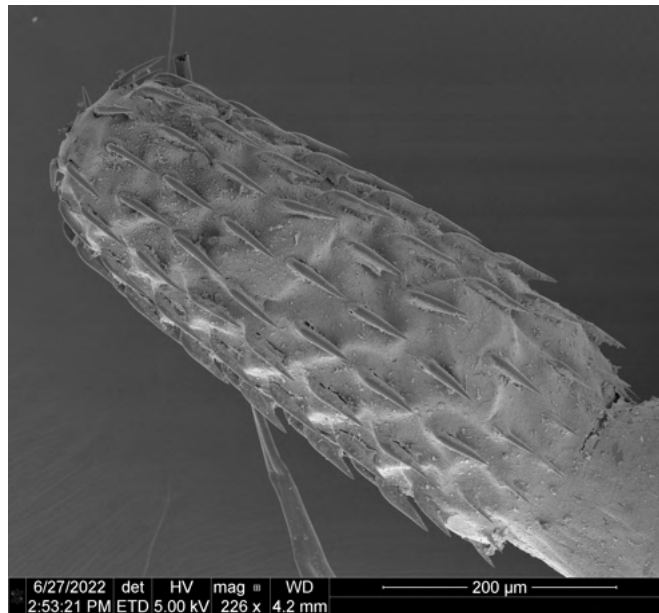
Figure 3.13 Lateral view of a fully everted proboscis from a female specimen of *A. dirus*.

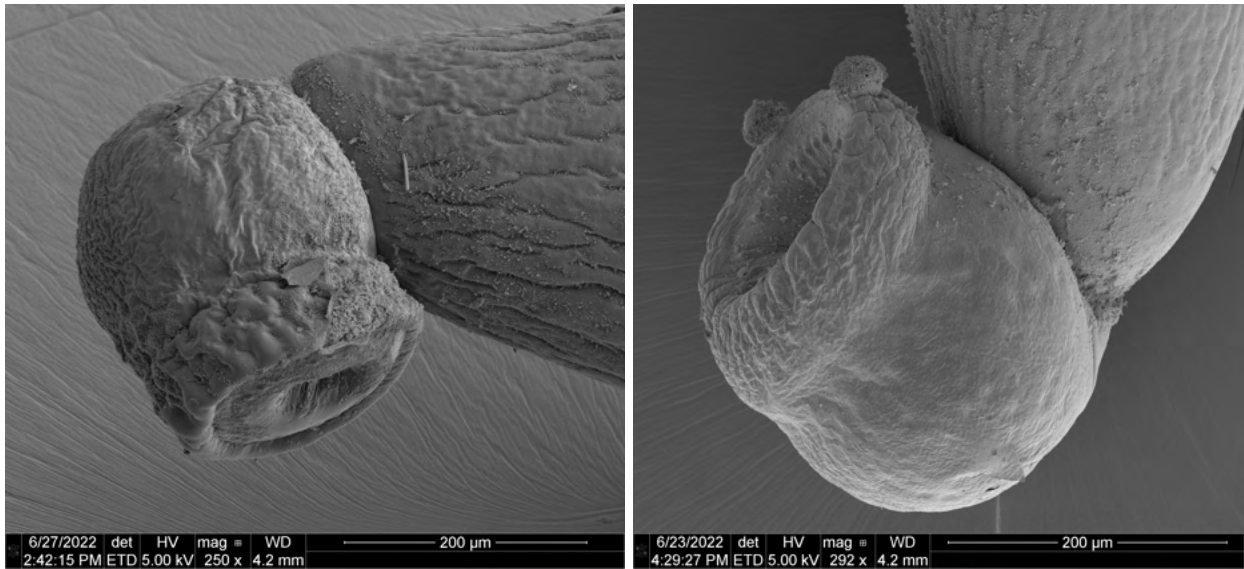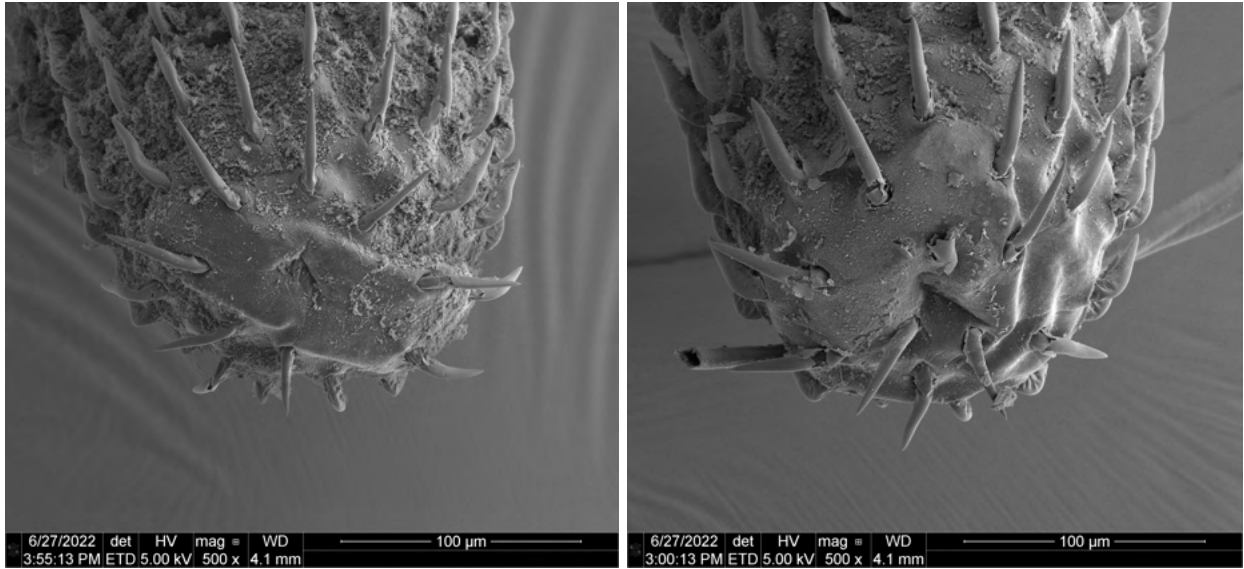**Figure 3.14** Anterior view of fully everted proboscides from female specimens of *A. dirus*.

Figure 3.15 Anterior view of a partially everted proboscis from a female specimen of *A. dirus*.

3.1.2.2 Hooks
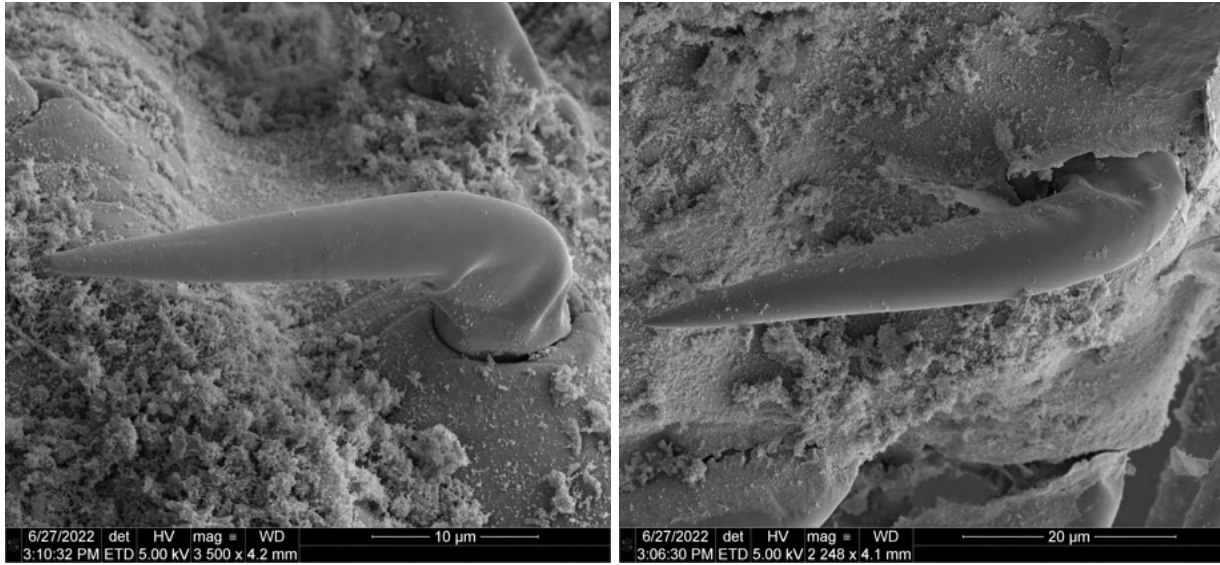
Figure 3.16 Lateral view of anterior hooks from female specimens of *A.dirus*.
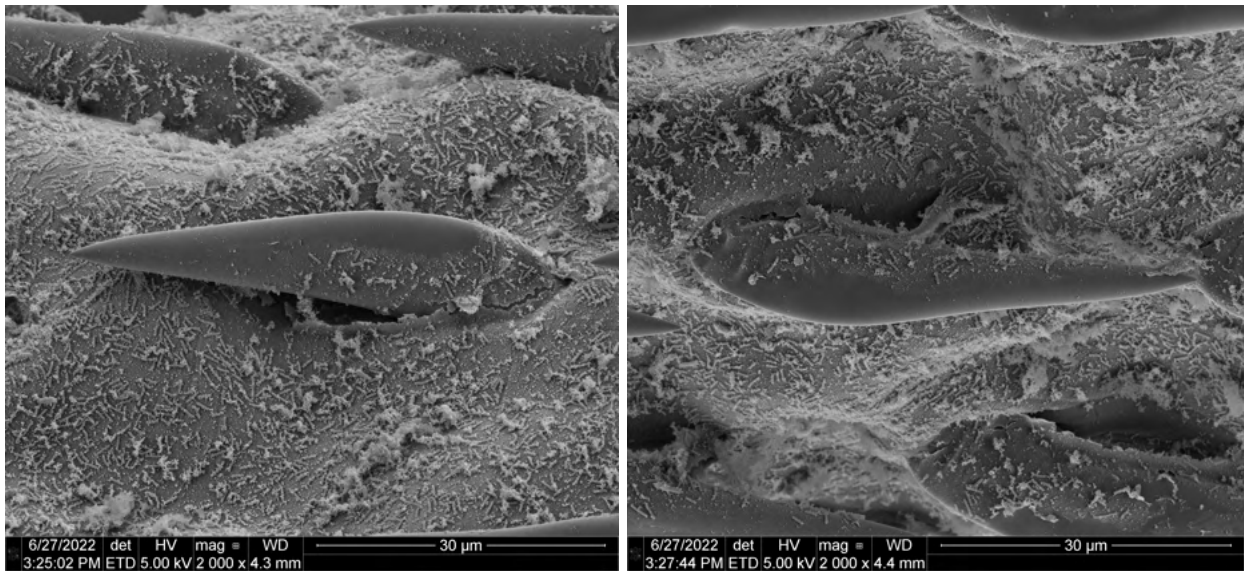
Figure 3.17 Lateral view of middle hooks from female specimens of *A.dirus*.
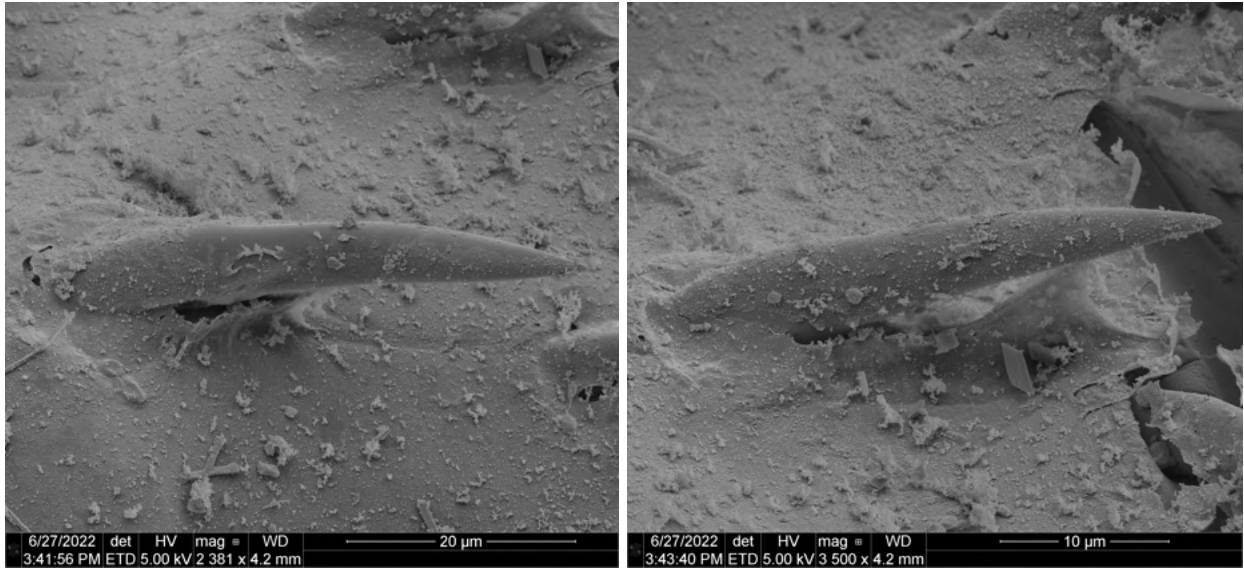
Figure 3.18 Lateral view of posterior hooks from female specimens of *A.dirus*.

    a.   Hook ornamentation
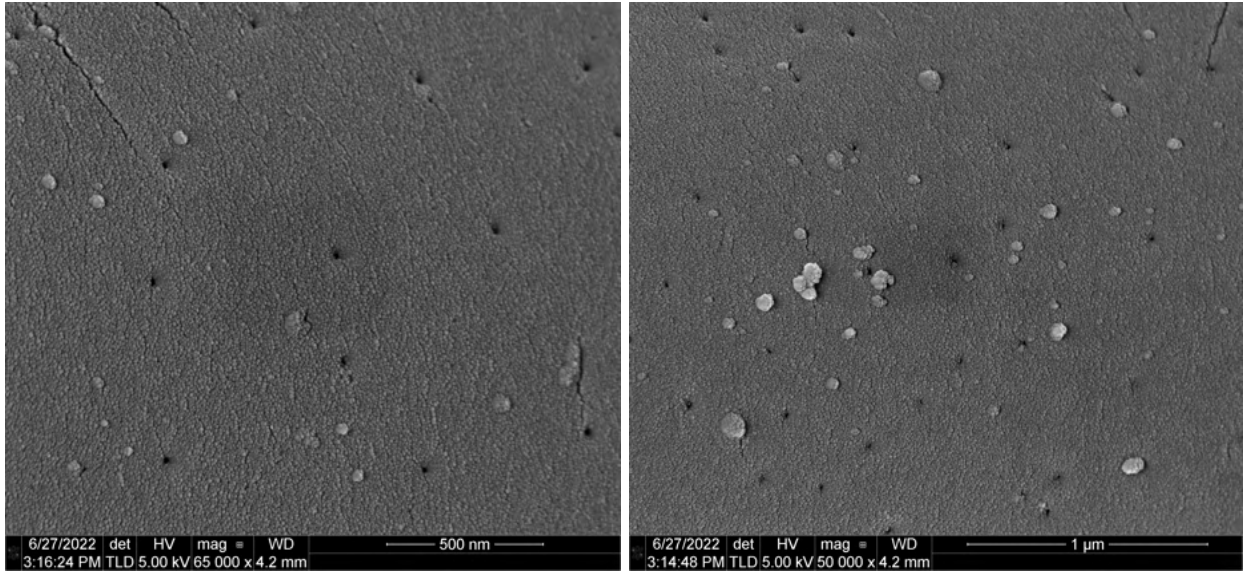
Figure 3.19 Images of hook pores identified on females. Their existence was unknown

previously.

3.1.2.3 Pores
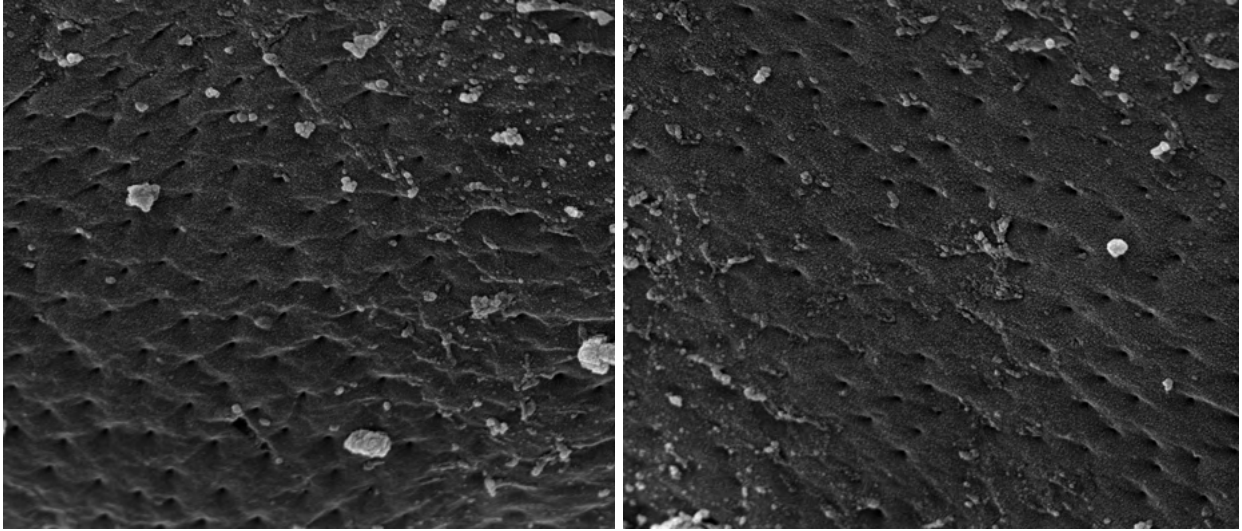
Figure 3.20 Pores on the proboscides of female specimens of *A. dirus*.

3.1.2.4 Gonopores
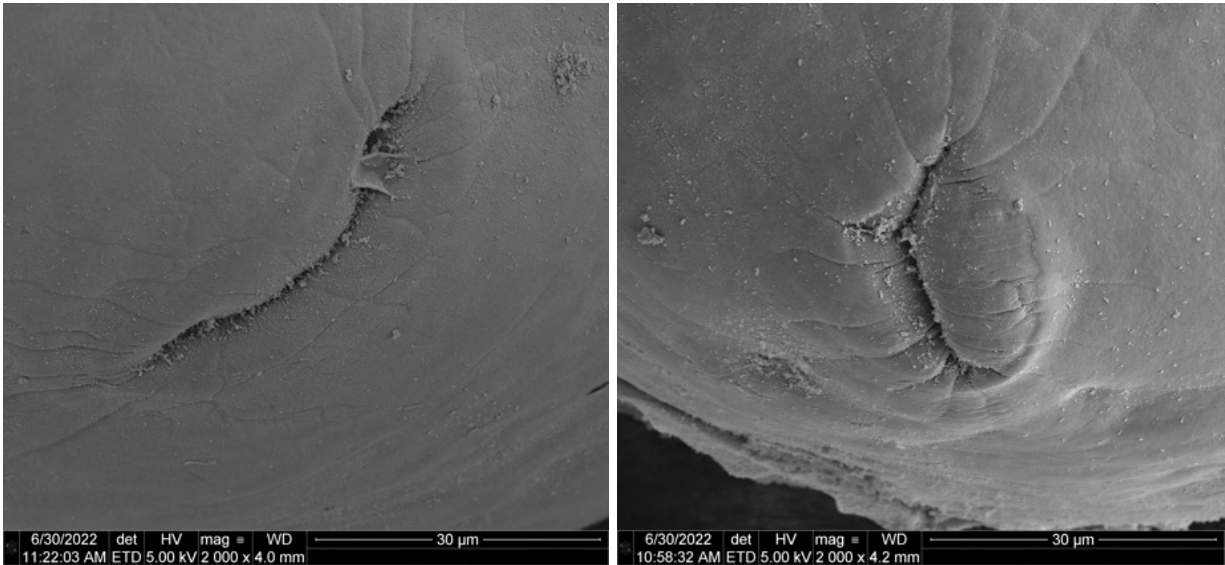
Figure 3.21 Gonopores on the posterior end of female specimens of *A. dirus*.

3.1.3 FIB and EDX data

The following tables provide the chemical analysis of different sections of the hooks on a female specimen of *A. dirus,* starting with the base of the hook all the way to the tip. The picture provides a better idea of the locations of analysis. Results are approximate.
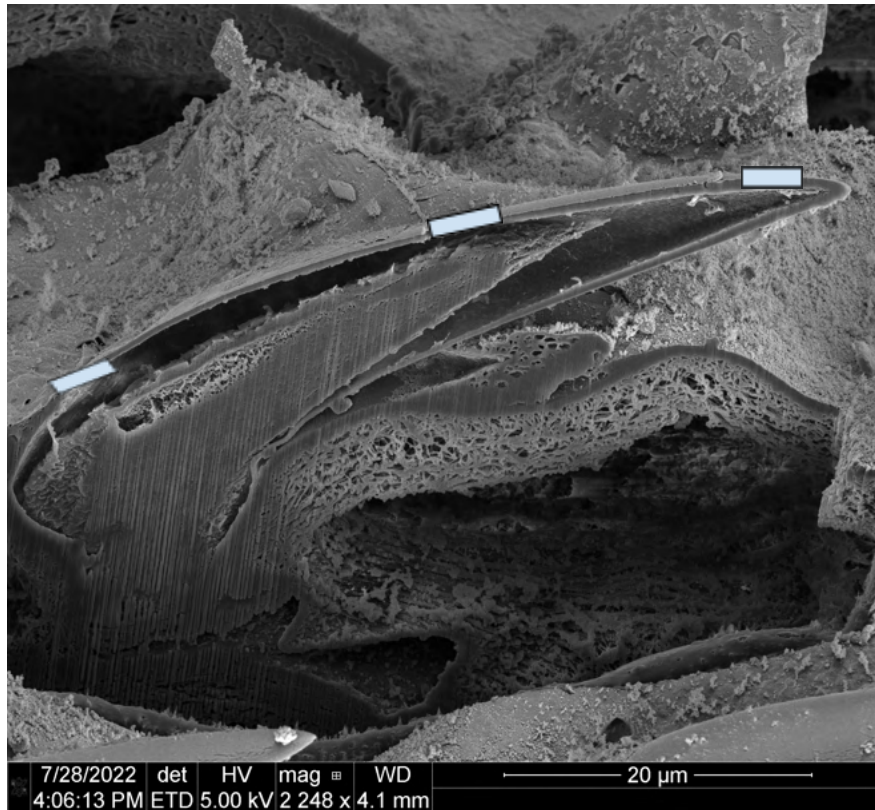
Figure 3.22 Longitudinal cross-section of a hook from a female specimen of *A. dirus*. The spectra below were taken at 3 different locations along the sheath (the outer cap) of the hook from the base to the tip.

Chemical composition of the middle of a hook from a specimen of *A. dirus*

Element	Weight %	Atomic %	Error %	Net Int.	K Ratio	Z	A	F
C K	19.79	40.42	99.99	237.44	0.09	0.977	0.4656	1

N K	11.63	20.37	12.7	129.56	0.0378	0.9539	0.3404	1
O K	12.1	18.55	9.62	227.41	0.0442	0.9346	0.3908	1
Na K	0	0	99.99	0.03	0	0.8536	0.6979	1.0004
Ga L	18.08	6.36	6.31	285.14	0.1318	0.6763	1.0784	0.9996
Mg K	0.06	0.06	99.99	1.98	0.0003	0.8708	0.6881	1.0004
Al K	2.55	2.32	11.36	92.78	0.0166	0.8413	0.7713	1.0009
P K	0.42	0.33	61.25	12.97	0.0031	0.8321	0.8969	1.003
Au M	14.77	1.84	9.94	193.3	0.1043	0.5484	1.2557	1.0254
S K	9	6.88	6.44	268.42	0.0688	0.852	0.8985	0.9988
Pd L	11.08	2.55	15.01	136.25	0.072	0.6405	1.0144	1.0001
K K	0.27	0.17	66.77	5.45	0.002	0.8181	0.9273	0.9977
Ca K	0.25	0.16	61.93	4.38	0.002	0.8377	0.9388	0.9977

Table 1. Chemical composition analysis of the base of a hook on a female specimen of *A. dirus*.

The table accounts for Au, Pd, and Ga introduced from sputter coating and FIB milling.
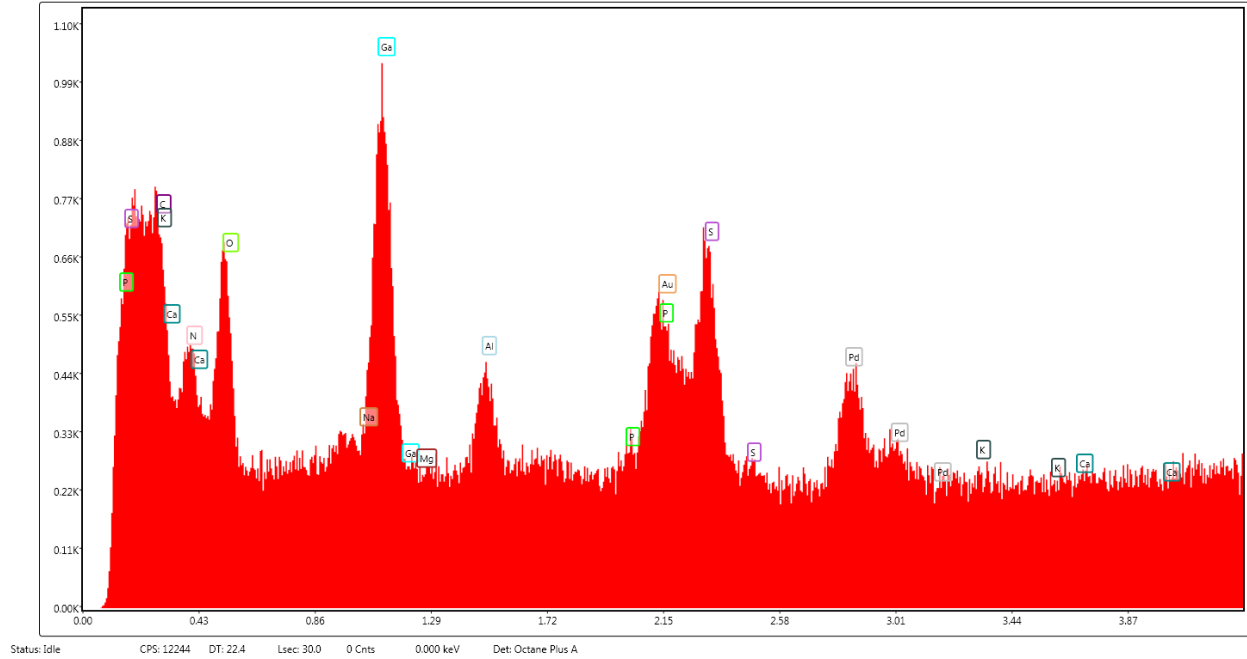
Figure 3.23 X-ray emission spectra from the base of a hook on a female specimen of *A. dirus*. The x-axis registers the photon energies while the y-axis registers the number of counts in thousands. Boxes indicate the characteristic lines of emission produced by the elements indicated.

Chemical composition of the middle of a hook from a specimen of *A. dirus*

Element	Weight %	Atomic %	Error %	Net Int.	K Ratio	Z	A	F
C K	16.69	39.61	99.99	197.76	0.0794	1.0098	0.4712	1
N K	9.34	19.01	13.34	97.87	0.0302	0.984	0.3288	1
O K	9.49	16.9	10.84	165.22	0.034	0.9628	0.3724	1
Na K	0	0	99.99	0.03	0	0.8773	0.6535	1.0002
Ga L	8.12	3.32	8.76	118.94	0.0582	0.695	1.0326	0.9999
Mg K	0.09	0.1	79.27	3.03	0.0006	0.8946	0.7142	1.0004
Al K	1.8	1.9	13.73	65.65	0.0124	0.8641	0.7992	1.0008

P K	0.43	0.4	60.88	13.23	0.0034	0.8546	0.9128	1.0029
Au M	24.52	3.55	8.83	310.14	0.1773	0.5633	1.258	1.0204
S K	11.59	10.3	6.23	329.9	0.0896	0.8751	0.8845	0.9985
Pd L	17.66	4.73	8.2	204.2	0.1143	0.6584	0.9837	1
K K	0	0	99.99	0.03	0	0.8413	0.8957	0.9967
Ca K	0.28	0.2	65.7	4.47	0.0022	0.862	0.9082	0.9965

Table 2. Chemical composition analysis of the middle of a hook on a female specimen of *A. dirus*. The table accounts for Au, Pd, and Ga introduced from sputter coating and FIB milling.

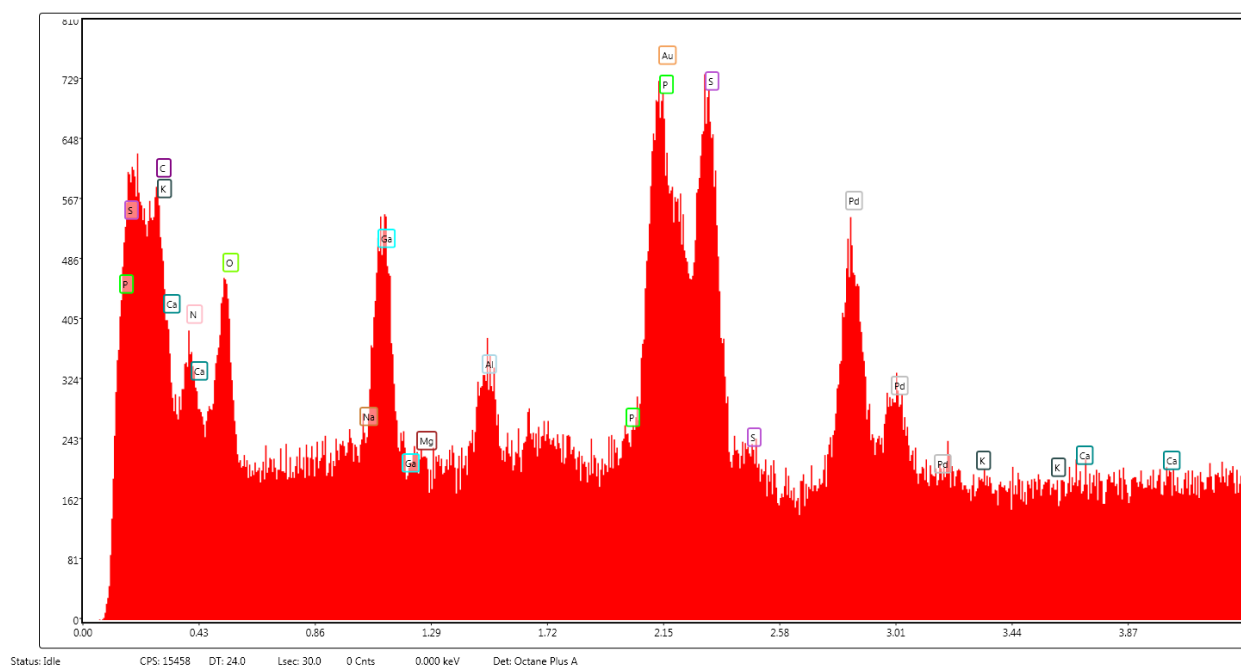**Figure 3.24** X-ray emission spectra from the middle of a hook on a female specimen of *A. dirus*. The x-axis registers the photon energies while the y-axis registers the number of counts in thousands. Boxes indicate the characteristic lines of emission produced by the elements indicated.

Chemical composition of the tip of a hook from a specimen of *A. dirus*

Element	Weight %	Atomic %	Error %	Net Int.	K Ratio	Z	A	F
C K	16.35	40.13	99.99	198.36	0.0657	1.0105	0.398	1
N K	7.44	15.67	14.74	88.26	0.0225	0.9845	0.3068	1
O K	7.04	12.97	11.15	145.88	0.0248	0.9634	0.3655	1
Na K	0.03	0.04	99.99	1.04	0.0002	0.8777	0.6605	1.0002
Ga L	6.23	2.63	9.33	112.05	0.0453	0.6954	1.0459	1
Mg K	0.08	0.1	77.76	3.38	0.0005	0.895	0.7317	1.0004
Al K	1.65	1.81	13.4	74.78	0.0117	0.8645	0.8152	1.001
P K	0.38	0.37	60.42	14.39	0.003	0.8549	0.9225	1.0033
Au M	23.53	3.52	8.38	367.12	0.1732	0.5635	1.2641	1.0331
S K	19.18	17.63	5.14	668.77	0.1498	0.8754	0.8936	0.9985
Pd L	17.82	4.94	8.26	247.36	0.1143	0.6586	0.9741	0.9998
K K	0	0	99.99	0.03	0	0.8415	0.8895	0.9968
Ca K	0.27	0.2	64.06	5.24	0.0021	0.8622	0.9035	0.9965

Table 3. Chemical composition analysis of the tip of a hook on a female specimen of *A. dirus*.

The table accounts for Au, Pd, and Ga introduced from sputter coating and FIB milling.

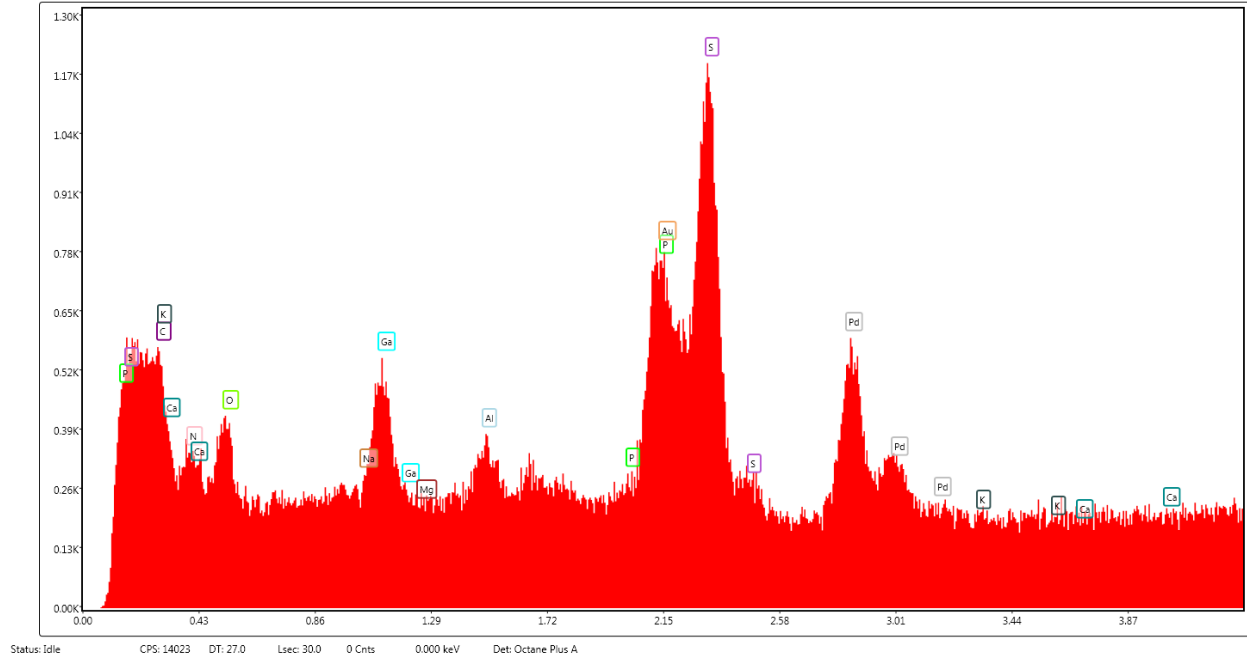**Figure 3.25** X-ray emission spectra from the tip of a hook on a female specimen of *A. dirus*. The x-axis registers the photon energies while the y-axis registers the number of counts in thousands. Boxes indicate the characteristic lines of emission produced by the elements indicated.

3.2 Discussion

The data provided above form a collection of pictures that expand the currently available description of *Acanthocephalus dirus*. They serve to strengthen the unification of *A. jacksoni*, *A. parksidei*, and *A. dirus* by displaying the identifying characteristics of this combined species in more detail than previously available. The measurements seen in the pictures fall within all the available ranges that were reported by Amin et al. (1975), Bullock et al. (1962), and Van Cleave et al. (1931) to describe the 3 previously distinct species and therefore serve as evidence to strengthen the decision to combine these species into one. Chemical composition determination via energy-dispersive X-ray analysis also serves this purpose by creating a dataset with which

future chemical composition analyses may be compared to determine the strength of the relationship between different specimens of the 3 previously distinct species.

3.3 Conclusion

The images set forth in this paper fulfill the purpose of this research by providing a more complete analysis and recharacterization of the parasitic thorny-headed worms of the species *Acanthocephalus dirus*. Although they have been described previously, the aid of scanning electron microscopy (SEM), energy-dispersive X-ray analysis (EDX), and focused ion beam (FIB) sectioning allowed for the production of a set of images and chemical analysis data that describe this species in more detail than previously possible. In examining the surface structures and composition of the specimens of this species, we created a dataset that provides more detail to any existing description of *A. dirus*.

Through this research, we have shed more light on the defining features of this species and identified its defining attributes to improve taxonomic definitions in the future. Further, we have outlined a procedure through which these SEM and EDX datasets can be consistently collected for comparison among other species of Acanthocephala to further aid in the taxonomy of the species. (or something like this)

References

Amin, O., Heckmann, R. & Ha, N. (2018). Descriptions of Acanthocephalus

parallelcementglandatus (Echinorhynchidae) and Neoechinorhynchus (N.) pennahia

(Neoechinorhynchidae) (Acanthocephala) from amphibians and fish in Central and

Pacific coast of Vietnam, with notes on N. (N.) longnucleatus. Acta Parasitologica, 63(3),

572-585. https://doi.org/10.1515/ap-2018-0066

Amin, O. M. (1975). Acanthocephalus parksidei sp. n. (Acanthocephala: Echinorhynchidae)

from Wisconsin Fishes. *The Journal of Parasitology*, *61*(2), 301–306.

https://doi.org/10.2307/3279010

Amin, O. M. (1984). Variability and redescription of Acanthocephalus dirus (Acanthocephala:

echinohynchidae) from freshwater fishes in North America. *Proceedings of the*

Helminthological Society of Washington, *51*(2), 255.

Bullock, W. L. (1962). A New Species of Acanthocephalus from New England Fishes, with

Observations on Variability. *The Journal of Parasitology*, *48*(3), 442–451.

https://doi.org/10.2307/3275212

Dalton, J. P. (2004). Role of the tegument and gut in nutrient uptake by parasitic platyhelminths.

Canadian Journal of Zoology, 82(2), 211-232. https://doi.org/10.1139/z03-213

Van Cleave, H. J. (1931). New acanthocephala from fishes of Mississippi and a taxonomic

reconsideration of forms with unusual number of cement glands. *Transactions of the*

American Microscopical Society, (59), 348–363.

Van Cleave, H. J., & Townsend, L. H. (1936). On the assignment of Echinorhynchus dirus to the

genus Acanthocephalus. *Proceedings of the Helminthological Society of Washington*, *3*,

63.